

H.-D. LANGER, H. G. SCHNEIDER

(Technische Hochschule Karl-Marx-Stadt, Sektion Physik –
Elektronische Bauelemente)

Stable Layer Systems with Diffusion Barrier Arrangements in Thin Film Technology

The physical and chemical interaction processes in thin film arrangements are followed by different ageing phenomena which influence the stability of their physical parameters. These determine the reliability of the electronic components existing of thin films.

On the base of own experimental investigations on tantalum and its oxides, beryllium oxide and tantalum-rhenium alloys technological aspects and the application of new materials for lowering the ageing intensity are considered.

Физическое и химическое взаимодействие в тонких плёнках приводит к различным феноменам старения, которые влияют на стабильность их физических параметров. Эта стабильность обозначает надёжность электронных приборов, которые состоят из этих тонких плёнок.

На основе своих экспериментальных исследований тантала и его окислов, окисла бериллия и сплавов тантала и рения, авторы рассматривают технологические аспекты и применение новых материалов для понижения интенсивности процессов старения.

1. Introduction

Though the classic materials for passive components of the microelectronic thin film technology, e.g. tantalum and its oxides, in many cases show the wanted properties, it became necessary to search for new and other materials, in order to guarantee a higher reliability and stability of such arrangements.

Therefore it was necessary intensively to investigate some important materials systems, just also Ta and its oxides, and especially BeO and Ta-Re-alloys ones, ageing mechanisms as well as their application in thin film capacitors and resistors LANGER (a), in order to find out how to stop or to diminish unwanted diffusion processes which negatively affect the stability and reliability of microelectronic components and circuits.

Without giving experimental details epitaxial growth, alloying and stable interlayers will be discussed in this connection since their application seems to be appropriate to improve the stability of thin layer systems in microelectronics.

2. Stability considerations of tantalum films

Tantalum layers are of high interest as base electrodes in thin film capacitors and as thin film resistors. The investigated Ta layers have been vacuum deposited by high vacuum electron impact evaporation (LANGER (b)). It is

typical for high melting metals, that their cohesive forces are higher than the adhesive ones, if they are deposited at $T \lesssim 450^\circ\text{C}$ on fused quartz. It results a high density of nucleus (FROMM, HÖFER), because of high cluster forming probability and a small number of atoms forming a nucleus of critical size results.

Under different formation conditions different Ta phases could be detected: *bcc* tantalum with lattice constants of 3,35 up to 3,50 Å (LANGER, MEYER, SCHNEIDER, LANGER (c)) tetragonal or β -Ta with $a = 4,4$ Å. β -Ta is metastable with respect to temperature and *fcc* Ta with respect to layer thickness. The transformation product always is *bcc* Ta. The transformation points — $T = 755^\circ\text{---}775^\circ\text{C}$ for β -Ta and $d = 300\text{---}500$ Å for *fcc* Ta — are very sensitive to film forming conditions (see also CHOPRA).

At room temperature deposited Ta films are always fine-crystalline independent on the bonding type and structure of the substrate. Figure 1 depicts a typical example.

Such films have been prepared on platinum grids and heated for a certain time (Δt_B) at stepwise elevated temperature in an electron microscope. Figure 2

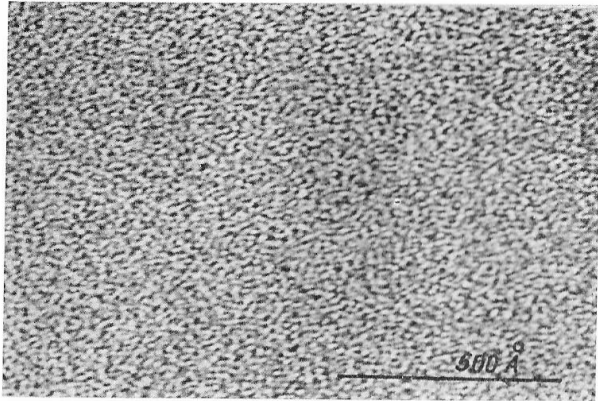


Fig. 1. Electron micrograph of a Ta film ($d = 300$ Å), deposited on (100) — NaCl at $T = 20^\circ\text{C}$

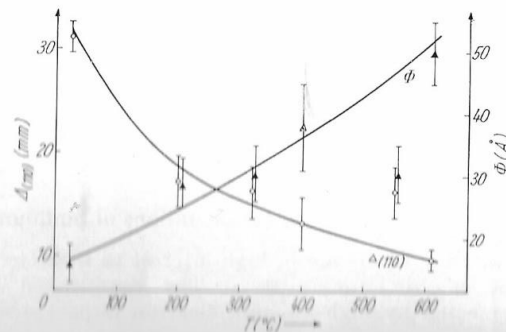


Fig. 2. Half width (Δ) of the (110) reflex and calculated grain diameter (ϕ , calibrated at $T = 20^\circ\text{C}$) of annealed Ta films as function of the annealing temperature

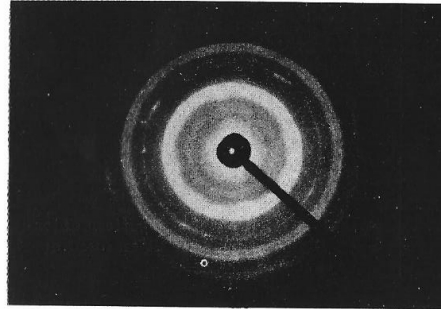


Fig. 3. Electron diffraction pattern of textured *bcc* tantalum condensed on (100) — NaCl at $T = 420^\circ\text{C}$ (β -Ta and β_1 -Ta₂O₅ also are present)

depicts the measured half-width of the respective electron diffraction rings. The calculated (stresses etc. are not considered) grain diameter is also shown in this figure. Thus the growth rate of this quantity is very small. With respect to recrystallization the same or a similar situation exists for a film undetached from and heated with the substrate. For producing more stable films with larger grain diameters it seems better to use directly the epitaxial condensation at a higher substrate temperature than to recrystallize a fine-crystalline film at the same temperature. For this the following arguments can be given:

- (i) The recrystallization duration is long with respect to the evaporation time. This causes a high quantity of impurities in the recrystallized films.
- (ii) Near the recrystallization temperature of high melting metals the films react with the substrate.
- (iii) Foreign atoms built in during heating increase the recrystallization temperature.

Because of a lack of careful experiments for the study of the film growth of high melting metals and their alloys from the lowest to a high thickness range the film forming mechanism is not yet completely understood. It seems that secondary nucleation because of high chemical reactivity, for instance similar to the situation of In films (Póczka), plays an important roll.

The growth of textured Ta films is possible on monocrystalline NaCl substrates at relative low substrate temperatures as shown in Figure 3. The possible intergrowth law for the *bcc* film is:



A very typical texture shows β -Ta even in fine-grained tantalum films (Fig. 4). This phenomenon we could not interpret. The formation of completely oriented monocrystalline films composed of *bcc* and tetragonal tantalum could be achieved on monocrystalline tungsten substrates (LANGER, MEYER, SCHNEIDER). The epitaxial relations were studied by means of X-ray and electron diffraction investigations. The relations are very simple:

1. $(110) [110]_{\text{bcc Ta}} \parallel (110) [110]_{\text{W}}$
2. $(100) [100]_{\beta\text{-Ta}} \parallel (110) [100]_{\text{W}}$

But the Ta-NaCl and also the Ta-W system are both only model systems and not applicable to thin film microelectronics. First investigations in the



Fig. 4. Electron diffraction pattern of textured β -tantalum condensed on fused quartz at $T = 400^\circ\text{C}$

authors' laboratory (LANGER (a); MEYER) of Ta films on insulating and semi-conducting substrates such as monocrystalline sapphire and silicon revealed the complexity of the problem, but also possible ways for the preparation of monocrystalline films.

It is supposed that in future more attention should be devoted to investigations combining structural, electrical, and other properties. This will be a successful way to find out the basic thin film phenomena. Such experimental procedures are for instance the study of structure and electrical resistance in-situ during the evaporation process or the investigation of the structure and temperature coefficient of electrical resistance during aging processes inclusive recrystallization, corrosion (especially grain oxidation), interstitial impurity solution, allotropic transformations, humidity effects etc.

In our laboratory such principles would be applied, but an exact analysis cannot be given here. Let us postulate here only a set of principal conclusions:

- (i) Tantalum films are very adhesive, mechanically hard, and stable against diffusion phenomena such like surface diffusion and electromigration. This implies that it is difficult to anneal any imperfections frozen in during deposition.
- (ii) Fine-grained tantalum films have a high free energy and therefore react very intensively with neighbored phases (substrate, other films, atmosphere).
- (iii) a) In most cases oxygen is present, and tantalum pentoxide is the most frequent aging product. But also other tantalum-oxygen phases (see for example Ta_2O (MÜLLER), nitrides (COYNE, TAUBER), hydrides (BERLINCOURT, BICKEL), silicides (JÄNGG et al.), carbides (FROMM, GEBHARDT, ROY) etc. could be observed. The reaction products are found on the surface and/or at the phase boundary substrate-deposit and are grown in the grain boundaries. The last process dominates with respect to its influence on the electrical properties.
b) Because of the defective lattice of the tantalum crystallites especially in as-grown, not tempered films more impurities are interstitially added than in the bulk. The solubility for oxygen is very high (LANGER (c)), but hydrogen, nitrogen and carbon present in oil diffusion pump vacuum systems also are soluble (RIEK, VOGEL; MORLEY, CAMPBELL).
- (iv) As a consequence of reaction and solution processes the electrical resistance rises (LANGER (a)), and this the more the thinner the as-grown

tantalum films are (see Fig. 5). In this way it is possible to overlap continuously the resistivity range corresponding to good conductors up to good insulators. At this point it must be stated that both the electrical resistivity (see Fig. 6) and its temperature coefficient (LANGER (c)) are dependent on the thickness.

It will be the subject of a further paper to discuss the reasons of these phenomena in detail. Despite the first one these basic considerations show

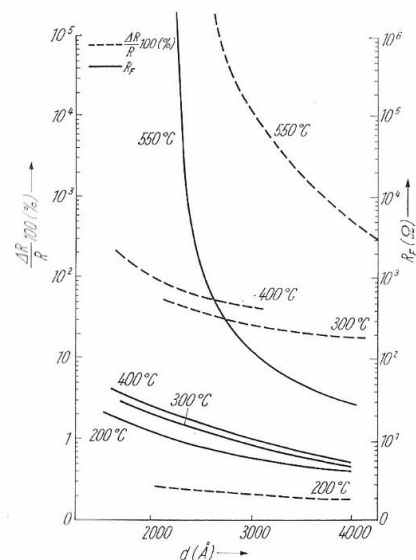


Fig. 5. Variation of electrical resistance $\left(\frac{\Delta R}{R}\right)$ 100 (%) and sheet resistance (R_F) of Ta foil as a function of thickness (d) at different annealing temperatures ($t_B = 100$ min in atmosphere)

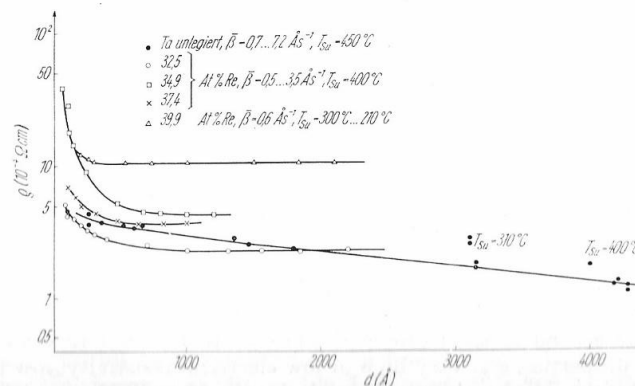


Fig. 6. Specific electric resistivity (ρ) of Ta films and Ta-Re films of different compositions as function of thickness, substrate temperature (T_{sub}), and mean evaporation rate (β); residual pressure during evaporation $4 \cdot 10^{-6}$ torr for Ta and $1 \cdot 10^{-5}$ torr for Ta-Re (see LANGER (d))

that fine-grained tantalum alone is not able to form stable thin film resistors. It must be embedded by insulating overlayers and/or underlayers which protect the metal against the atmosphere and chemically unstable adjacent phases. Such layers have to be chemically very stable and to act as diffusion barrier against any reactant or diffusant in thermal and/or electric fields (DALTON, DROBECK). But alloying and/or growth controlled machining of large-crystalline Ta films are also possible ways.

In the next chapters the three general ways cited for the realization of more stable tantalum base film structures will be considered.

3. Epitaxial growth

Because the total oxygen uptake ability (oxygen is atomic at interstitials and chemically bounded at grain boundaries) decreases with increasing grain size, i.e. decreasing free grain boundary energy, it would be necessary to prepare epitaxial monocrystalline films. This is a difficult technical problem, as we have already shown, but we think that the stability would be remarkably increased if one applies films with grain diameters of 0.1–1.0 μm instead of 20–500 \AA , produced by epitaxial growth on polycrystalline or monocrystalline substrates.

4. Alloying

Multicomponent materials often have the advantage of higher variability of their properties. Thus alloying is also an extremely fine method to produce stable films.

Two ways are possible:

- (i) Heterogeneous alloying of the tantalum (or related transition metals like Nb, Ti, Zr etc.) with noble metals like Au, Ag, Pd, and Pt filling up and deactivating the grain boundaries: Ta–Au alloy films of this type have an extremely high stability in atmosphere at temperatures up to 400 °C (MAISSEL). The only, but deciding disadvantage of this technique are the high material costs.
- (ii) Homogeneous alloying with transition metals for lowering the interstitial solubility of oxygen, hydrogen, and other atomic species: Based on the calculated band structure of various transition metals (MATTHEISS 1965, 1970), the validity of the rigid band model, and the prediction, that the solved oxygen behaves metallicity and donates an electron to the free electron gas (CHAO, ANSELL), one of the authors (LANGER (d)) recently has predicted the composition ranges of binary transition metal alloys with zero solubility for oxygen and hydrogen. These alloy compositions are given in Table I. Experimental results on tantalum–rhenium alloys have shown the occurrence of this electron-structure effect also in thin films.

The second method offers possibilities to find out new materials with new properties, e.g. very high or low electrical resistivity, low temperature coefficient of the electrical resistivity or high hardness. The thickness (see Fig. 6) at which the electrical resistivity becomes independent on the thickness, is relatively low and independent on the alloy composition. These are important assumptions for a high reproducibility.

Table I
Predicted composition of binary alloys of the group IV and group V metals and of binary alloys of this metals with group VI, VIII, and VII metals to obtain zero hydrogen and oxygen solubility (LANGER (d))

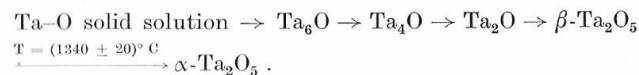
Binary alloy of group	Composition (at %)	
IV – VI	5...20	} IV-metal
IV – VIII	37...47	
IV – VIII	52...60	
V – VI	10...40	} V-metal
V – VII	55...70	
V – VIII	60...70	

The Ta–Re system has advantages in co-evaporation because of neighbouring melting temperatures and vapour pressures. The lower formation energy of the oxides of the higher melting alloy components and the lower diffusion mobility of the other ones are also favourable conditions for alloy films resistant to ageing in oxygen atmosphere. For many alloys mentioned in Table I this condition is satisfied.

5. Insulating diffusion barrier layers

A technologically simple case would be the thermal oxidation. In microelectronics the Si–SiO₂ system has been frequently realized in this way. Therefore at first consideration is given to interaction of oxygen with tantalum.

Both the authors have reported on the system tantalum–oxygen in a concentrated paper three years ago (SCHNEIDER, LANGER). There, the special significance of the high oxygen solubility of tantalum as to reaction mechanism, reaction kinetics, and phase equilibrium has been accentuated. It is characteristic for the bulk material that there are an internal and an external reaction zone. With increasing oxidation period and temperature of reaction, as well as increasing oxygen partial pressure the following transformations take place in the phase boundary region (COWGILL):



$\beta\text{-Ta}_2\text{O}_5$ is the stable modification of tantalum pentoxide in the low temperature range. The structure of $\beta\text{-Ta}_2\text{O}_5$ is orthorhombic. Figure 7 depicts a model of the atom arrangement in the elemental cell. Further polymorphs of Ta₂O₅ are cited in the literature (SCHNEIDER, LANGER).

In the temperature range of 20 °C up to 450 °C an amorphous oxide is formed on the surface of bulk tantalum. This amorphous oxide is transformed to crystalline tantalum pentoxide under the influence of an electric field or after longer annealing in this temperature range. Below the amorphous oxide layer Ta_nO phases are formed at P_{O₂} = 760 Torr and T ≥ 300 °C (COWGILL; VERMILYEA). Crystalline $\beta\text{-Ta}_2\text{O}_5$ can be observed from T ≥ 450 °C. At first from T = 200 °C a noticeable reception of oxygen in tantalum can be measured (KOFSTAD 1963) and nearly at the same temperature the growth of the surface

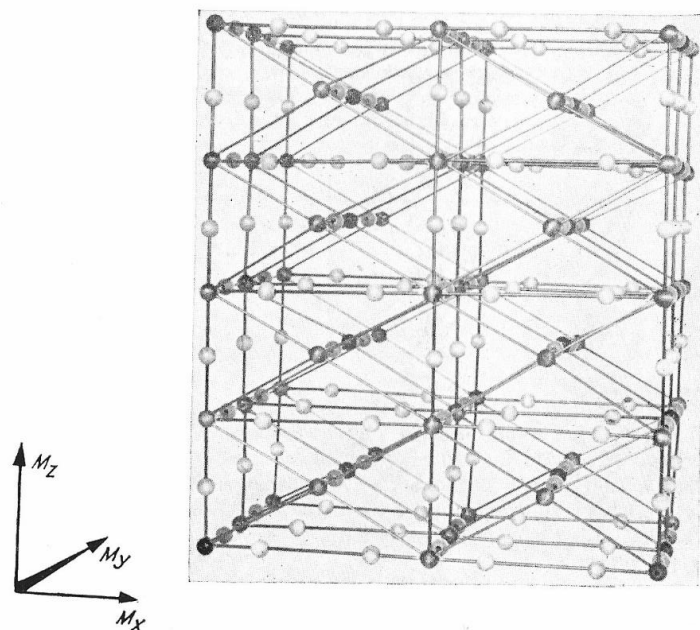
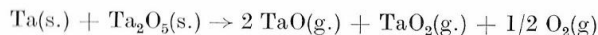


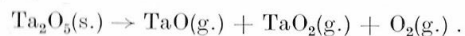
Fig. 7. Model of the β - Ta_2O_5 structure ($a = 6,20 \text{ \AA}$, $b = 3,66 \text{ \AA}$, $c = 3,89 \text{ \AA}$ (LEHOVEC 1964): White balls = oxygen, black balls = tantalum

oxide layer essentially increases (GULBRANSEN, ANDREW). The oxygen migrates in tantalum through octahedral interstices. The activation energy is $25,5 \text{ kcal mole}^{-1}$ at $T = 400 \text{ }^\circ\text{C}$ (SCHNEIDER, LANGER).

The degassing of a Ta/O solid solution in high vacuum is effected by the evaporation of TaO and TaO_2 (HÖRZ). In the vapour space of Ta/ Ta_2O_5 mixture Ta_2O_5 molecules cannot be found at high temperatures, but those of TaO and TaO_2 (GorošČENKO). Ta_2O_5 is not stable under these conditions and reacts with Ta:



and/or disproportionates:



Therefore it is not possible to prepare stoichiometric Ta_2O_5 -films by the aid of direct evaporation of Ta_2O_5 , but in an O_2 -atmosphere ($P_{\text{O}_2} = 10^{-4} \dots 10^{-1}$ torr dependent on evaporation rate and reactivity coefficient) corresponding to the latter equation, if the reverse reaction takes place on an appropriately heated substrate.

Not too much is known about the phases Ta_nO with $n > 1$, because it is difficult to prepare samples sufficient in size. Perhaps they are of a more intermetallic compound character rather than heteropolar. The best argument for this is the metallic character of the interstitially solved oxygen. The screening model of ANSELL and CHAO (look Chapter 3) holds only for the case

free of interaction. The interaction of oxygen atoms in the oversaturated ranges may activate the ordering processes leading to the Ta_nO formation. Further investigations are necessary to prove this model.

Bulk tantalum coexists with its oxides in an unlimited oxygen container only in a dynamic equilibrium. The temperature, pressure and time dependent reaction processes always lead to the final product β - Ta_2O_5 at $T < 1340 \text{ }^\circ\text{C}$. Figure 8 depicts the temperature dependent oxidation rate (linear rate law) of bulk tantalum at $P_{\text{O}_2} = 760$ torr.

It is not unreasonable to speak of the thin film state as a special state of matter with properties often very different from the bulk. For thin fine-grained films this is especially valid. The question is whether the free energy of this system is such that remarkable differences relative to the bulk tantalum may be detected in thermal oxidation. We compared the thermal oxidation of polycrystalline tantalum sheets and of tantalum films evaporated on fused quartz and on monocrystalline NaCl substrates.

Electronmicroscopic in-situ studies of thermal oxidation (short time oxidation at step-by-step elevated temperature at different oxygen partial pressures) have been performed with tantalum films floated off from NaCl in aqua dest. and prepared on heatable platinum grids. The occurring Ta-O phase detected by electron diffraction are cited in Figure 9. The related X-ray data are given by MIRKIN for β_1 - Ta_2O_5 , LEHOVEC (1964) for β - Ta_2O_5 , KOFSTAD 1964 for α - Ta_2O_5 ,

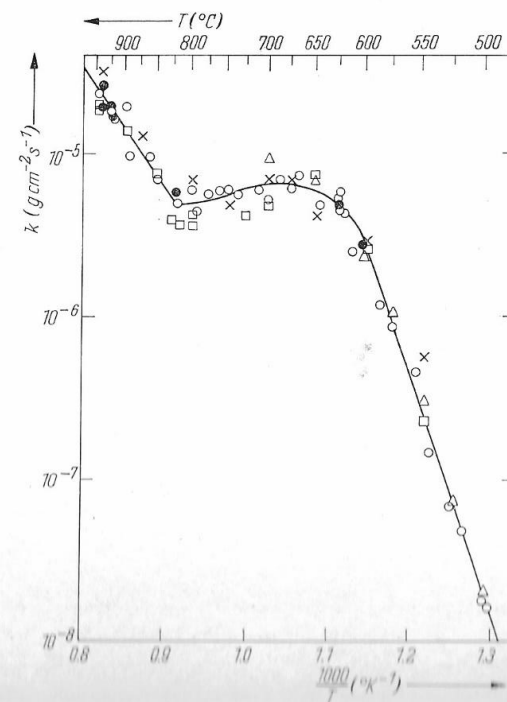


Fig. 8. Oxidation rate (k) of tantalum (linear rate law) in atmosphere as a function of temperature t (in $^\circ\text{C}$) respective reciprocal absolute temperature

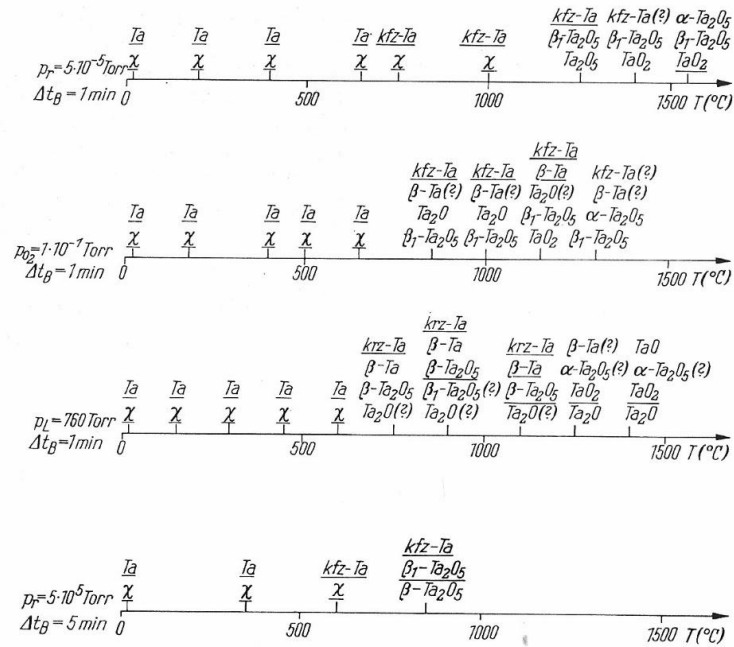


Fig. 9. The various phases in and on thin Ta films in different environments ($d_{Ta} = 300 \text{ \AA}$): $\text{Ta} \triangleq \text{fcc Ta}$ (with overlapped (110) and (200) reflexes), $\chi \triangleq$ amorphous tantalum oxide, $\text{kfz-Ta} \triangleq \text{fcc Ta}$, $\text{krz-Ta} \triangleq \text{bcc Ta}$, $P_r \triangleq$ residual pressure, $P_L \triangleq$ atmospheric pressure

SCHÖNBERG for TaO (cubic) and TaO₂ (tetragonal), NORMAN for Ta₂O (tetragonal), STEEB, RENNER; URASALIEV for Ta₂O (cubic).

As an example Figure 10 shows a set of electron diffraction patterns of a tantalum film annealed in air. The intensive diffraction ring in the patterns

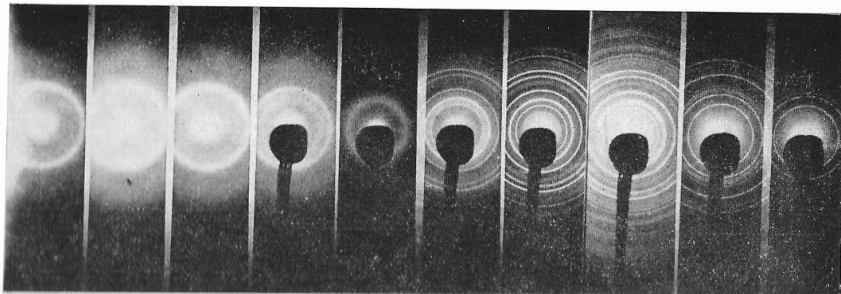


Fig. 10. Electron diffraction patterns of a Ta film annealed step by step in atmosphere ($d_{Ta} = 300 \text{ \AA}$): $T_1 = 20 \text{ }^{\circ}\text{C}$, $T_2 = 150 \text{ }^{\circ}\text{C}$, $T_3 = 300 \text{ }^{\circ}\text{C}$, $T_4 = 450 \text{ }^{\circ}\text{C}$, $T_5 = 620 \text{ }^{\circ}\text{C}$, $T_6 = 750 \text{ }^{\circ}\text{C}$, $T_7 = 920 \text{ }^{\circ}\text{C}$, $T_8 = 1100 \text{ }^{\circ}\text{C}$, $T_9 = 1250 \text{ }^{\circ}\text{C}$, $T_{10} = 1400 \text{ }^{\circ}\text{C}$

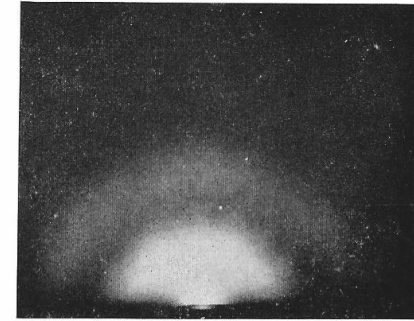


Fig. 11. Reflection electron diffraction pattern of amorphous thermal tantalum oxide prepared at $T = 200 \text{ }^{\circ}\text{C}$ in atmosphere ($\Delta t_B = 3 \text{ h}$)

a) to d) is typical for fine-grained tantalum. In pattern d) at first the diffuse ring of an amorphous oxide (phase χ in Fig. 9) is clearly visible. The underlined phases in Figure 9 fulfilled the X-ray data best. In the other cases some rings were absent or the relative intensities differed strongly. The phases therefore in question are furnished with a mark of interrogation. We have performed long time oxidation experiments on Ta films (LANGER (a)) up to a temperature of $500 \text{ }^{\circ}\text{C}$. The thickness increase of the oxide film obeys a parabolic law.

The oxide films are completely amorphous as reveals the reflection electron diffraction pattern in Figure 11. With increasing temperature and time the diffuse ring reflexes become sharper as a consequence of progressive ordering processes in the oxide layer. The applicability of such films as dielectrics and diffusion barriers is limited by cracking. The blister-like beginning of this process after annealing for four hours at $T = 500 \text{ }^{\circ}\text{C}$ in air is depicted in Figure 12. We deposited gold films on top of the oxide in order to investigate their electronic properties in a capacitor structure with a Ta film as basic electrode and the Au film as counter electrode. The result was surprising. Employing the well known plate capacitor formula we calculated an amount

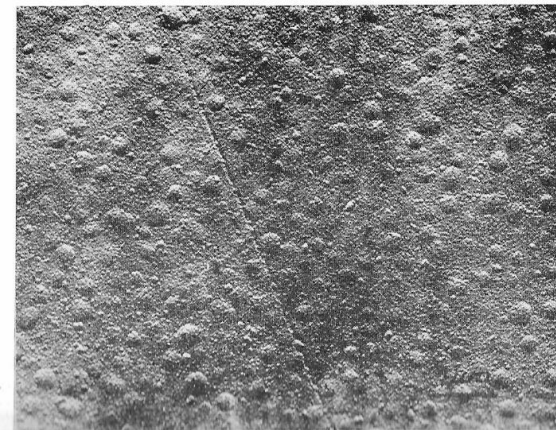


Fig. 12. Blister-like cracking of thermal tantalum oxide revealed by an electronmicroscopical C-Pt replica

Table 2
Lattice plane distance (d_{hkl}) and related millers indices (hkl) of various tantalum oxides estimated by X-ray diffraction by different authors

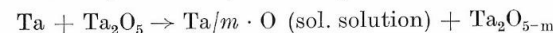
β_1 -Ta ₂ O ₅ (MIRKIN)	β_1 -Ta ₂ O ₅ (LEHOVEC 1964)		α -Ta ₂ O ₅ (KOFSTAD 1964)	TaO (SCHÖNBERG) (cubic, $a = 4,43 \text{ \AA}$)		TaO ₂ (SCHÖNBERG) (tetragonal $a = 4,709 \text{ \AA}$ $c = 3,065 \text{ \AA}$)
$d_{hkl}/\text{\AA}$	$d_{hkl}/\text{\AA}$	hkl	$d_{hkl}/\text{\AA}$	$d_{hkl}/\text{\AA}$	hkl	$d_{hkl}/\text{\AA}$
6,2	3,87	001	3,75	2,56	111	3,34
5,7	3,15	110	3,59	2,21	002	2,58
4,48	3,09	200	3,34	1,73	022	2,36
3,96	2,45	111	3,03	1,47	113	1,74
3,49	2,42	201	2,96	1,28	222	1,67
3,23	1,94	002	2,73	1,11	004	1,53
3,05	1,83	020	2,45	1,02	133	1,49
2,95	1,79	310, 112	2,33	0,99	024	1,39
2,81			2,22	0,90	224	
2,61	1,65	021, 202	2,10			
2,45			2,01			
2,29	1,63	311	1,89			
2,15	1,58	220	1,84			
1,98	1,55	400	1,78			
1,87	1,46	221	1,69			
1,77	1,44	401	1,65			
1,66	1,32	312	1,58			
1,62	1,22	322	1,55			
1,71	1,33	022	1,60			

Table 2 (continued)
Ta₂O

(tetragonal, $a = 6,680 \text{ \AA}$, $c = 4,758 \text{ \AA}$) (NORMAN)		(cubic, $a = 6,68 \text{ \AA}$) (STEEB, RENNER)		(cubic, $a = 6,68 \text{ \AA}$) (URASALIEV)	
d_{hkl}	hkl	d_{hkl}	hkl	d_{hkl}	hkl
4,72	110	4,72	110	6,68	100
2,72	201	2,73	112	3,26	200
2,52	211	2,23	300	2,37	220
2,23	300, 102	2,12	310	2,01	311
2,11	310, 114, 221	2,02	311	1,41	332
2,01	301	1,93	222	1,185	440
1,93	311, 202	1,58	330	0,885	642
1,57	330, 401, 312	1,46	421		
		1,43	332		
		1,31	510		

of the relative dielectric constant ϵ of 200 and more. This amount is by one order of magnitude greater than the related amount of the bulk oxide (PAVLOVIĆ) and of thin amorphous anodic oxide films (YOUNG). It will be the subject of the further paper to discuss this phenomenon in detail under the point of

view of polarization mechanisms. But in principle our consideration is based on an oxygen deficiency model of the amorphous tantalum oxide film. It is normal, also for anodic oxide films, that during the growth process point defects are built in. In the case of thermal tantalum oxide these may be oxygen vacancies and interstitials (KOFSTAD 1962). The oxygen interstitials may be concentrated in a small zone at the oxide/oxygen boundary during oxidation. But at the boundary tantalum/oxide we postulate a chemical reaction.



leading to a characteristic vacancy profile in the oxide. According to (SMYTH, SHIM) and (LEHOVEC 1968) there is an exponential decrease of the amount of oxygen vacancies in annealed anodic oxide films adjacent to bulk tantalum

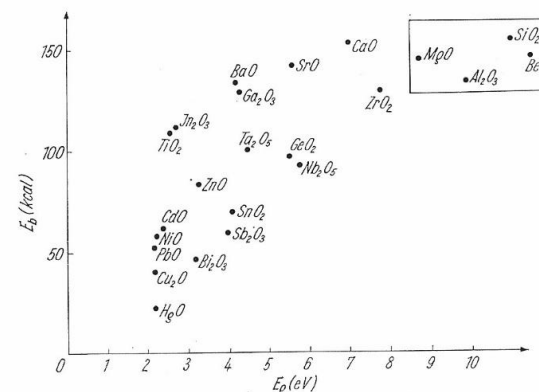


Fig. 13. Dissociation energy per g -atom of oxygen (E_b) of some oxides as a function of band gap (E_g)

from the phase boundary to the oxide surface. The driving force may be the remarkable difference in dissociation energy per oxygen atom of Ta₂O₅ (see Fig. 13) and the solution enthalpy of oxygen in tantalum (148 kcal per g -atom for the bulk (STRINGER)). The chemical interaction in our thin film systems with fine-grained tantalum films was more typical than in the bulk tantalum case.

This chemical nonequilibrium situation excludes the practical applicability of thermal amorphous tantalum oxide as diffusion barrier on fine-grained tantalum films. Concluding we have to reduce the oxygen deficiency of the oxide. This may be achieved

- (i) by doping the oxide with ions which effect the defect equilibrium and/or diminish the diffusivity of the active species like phosphorus ions in amorphous tantalum oxide films (SMYTH, TRIPP, SHIRN) or dysprosium ions in glassy films (HACSKAYLO, SMITH), or lowers the electronic conductivity
- (ii) by employing crystalline oxide films prepared by other methods than thermal oxidation operating at relative low temperatures, e.g. anodic oxidation (MOHLER, HIRST; MANASEVIT, FORBES, CADOFF) and

(iii) by lowering the reactivity of the underlying tantalum film as described in chapters 3 and 4.

Furthermore we have the possibility to use other insulating materials which combine excellent protective properties with high chemical stability. But the accepted film forming method must be compatible with modern vacuum technology in the microelectronic technology. Evaporation and sputtering are such methods in which the material is transported monomolecularly or as small molecular clusters from the source to the substrate through the vapour room. This requires a low dissociation ability as a further condition. Figure 13 depicts the dissociation energies per oxygen atom of some oxides in dependence on the band gap. The most stable oxides which are appropriated for our purposes are framed. Ordering and reaction processes in the layer on the substrate for improving the stoichiometry were the more activated the higher the free formation energy of the deposit is. Figure 14 depicts the temperature dependence of the standard free formation energy of some compounds.

In general it is desirable to have low electrical and high thermal conductivity and a high thermal expansion coefficient. Dependent on temperature these values are given for some interesting bulk compounds in Figure 15 to Figure 17. According to MAISSEL there are indications that dielectric losses of the most oxides decrease with increasing band gap.

Indeed, the number of listed physical and chemical properties and cited compounds is very limited but the detected trends allow us to choose some compounds which from this point of view are well applicable, e.g. MgO, BeO, Al_2O_3 , SiO_2 , HfO_2 . Beryllium oxide is an excellent representative of this group. Little is known in the literature about structure, diffusion barrier, and electronic properties of BeO films, though this material has wide applications in nuclear technique, ceramic industry and classical electronic. Also in microelectronics applications as substrate (MANASEVIT) and as insulating intermediate layer in integrated circuits are already known (SETO). The toxicity problem is well

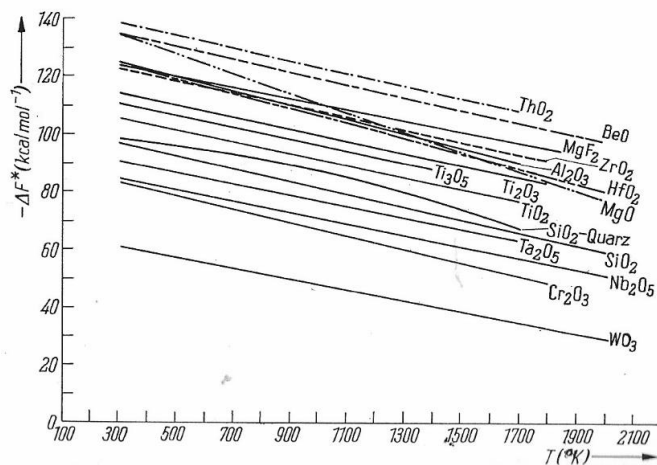


Fig. 14. Standard free energy of some compounds as a function of temperature

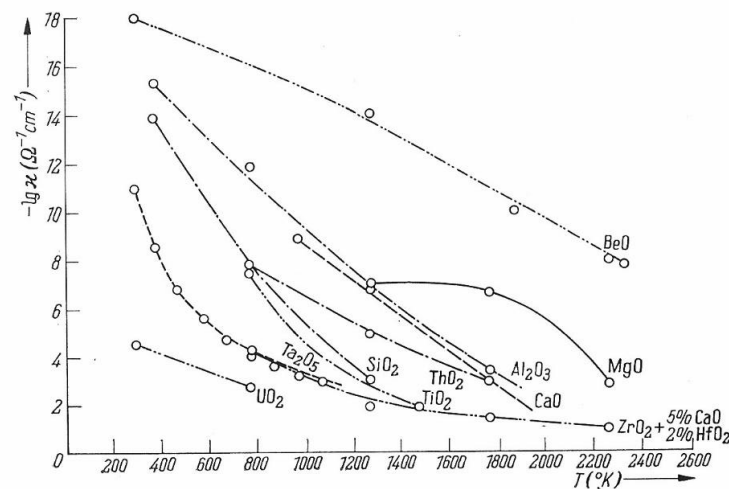


Fig. 15. Electric conductivity of some oxides (logarithmic plot) as a function of temperature

governed and the related operating conditions are compatible with the general clean room ones in the microelectronic industry (KRIVSKY; MÖNCH). Therefore we have investigated the relations between structure, physical properties, and ageing mechanisms of vacuum evaporated BeO films (LANGER (a)). We have not found any data for such films in the literature. Detailed experimental results are to be published in a next paper. In chapter 6 we only give a short review.

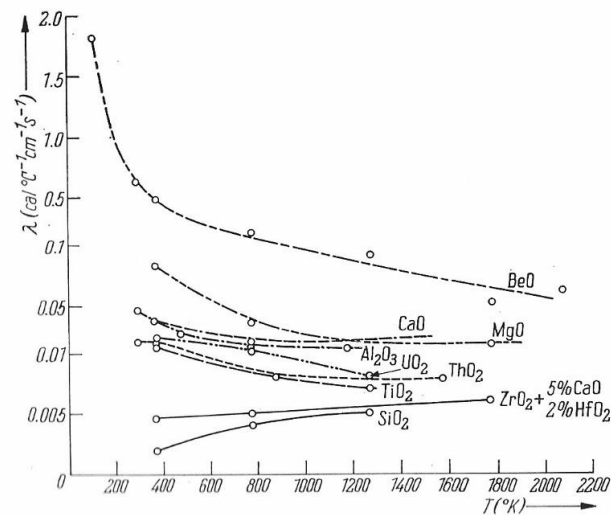


Fig. 16. Thermal conductivity of some oxides as a function of temperature

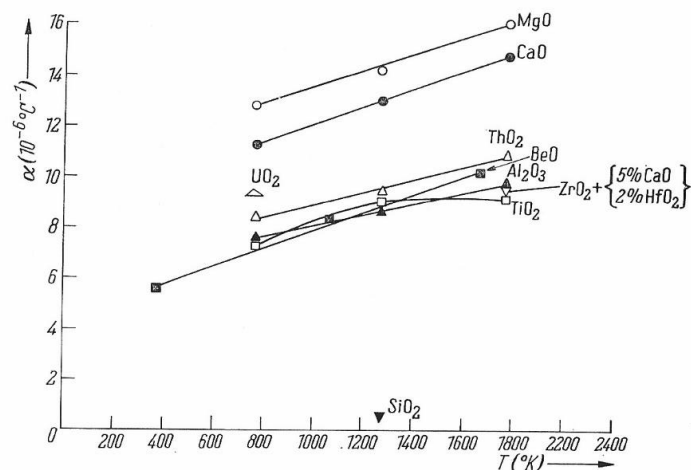


Fig. 17. Thermal dilatation coefficient of some oxides as a function of temperature

6. Beryllium oxide

Because of the high bonding strength of beryllium oxide (see Fig. 13) the BeO molecule is stable in the vapour space (HAUSNER). Therefore the compound-evaporation is applicable (FRELLER). The temperature dependence of the vapour and the dissociation pressures on BeO are depicted in Figure 18. To attain a deposition rate of, for instance, 100 \AA s^{-1} it is necessary to evaporate at the melting temperature $T_s = (2540 \pm 10)^\circ\text{C}$ or at higher temperatures.

Our evaporating source was a tungsten boat carefully shielded to minimize the hot tungsten surface optically visible at the substrate. But other techniques are available, for instance laser beam, xenon light, and electron beam evapora-

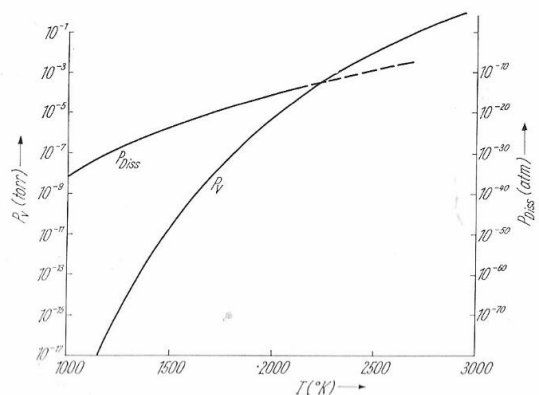


Fig. 18. Vapour and dissociation pressures of beryllium oxide as a function of temperature

tion, ion beam, Rf-, and reactive sputtering, anodic or thermal oxidation, pyrolysis and chemical transport reactions.

In order to prove the existence of the valence vibration band as a proof for the chemical BeO bond vapour deposited layers and the powdered vapour source material were investigated by infrared spectroscopy. The layers were deposited at $T = 20^\circ\text{C}$, at an evaporation rate of 100 \AA s^{-1} , and at a residual vapour pressure of $5 \cdot 10^{-6}$ torr on monocrystalline NaCl substrates. The thickness was 3000 \AA . The powdered crystalline material shows splitted spectra because of the wurtzite crystal symmetry with absorption maxima at $k = 880 \text{ cm}^{-1}$ and 760 cm^{-1} . The only absorption maximum of the film lies exactly in the middle at $k = 810 \text{ cm}^{-1}$ indicating the amorphous state and the presence of the BeO valence bond. The layer spectra do not show the satellite minima, which are visible in the powder spectra indicating their higher purity.

Well textured BeO layers could be deposited upon monocrystalline tantalum slices. The intergrowth law is



and it may be possible to prepare complete monocrystalline layers. The lattice constants of the Wurtzite type $\alpha\text{-BeO}$ are $a = 2,698 \text{ \AA}$ and $c = 4,378 \text{ \AA}$ (AUSTERMANN).

It could be proved that thin amorphous BeO layers deposited upon fine-grained tantalum resistors are excellent barriers against thermal and field drift of tantalum oxygen.

Ageing processes in high vacuum up to temperatures of 500°C show the low phase boundary reactivity between both layers. Also the electronic and dielectric properties measured in thin film capacitor arrangements show remarkable relations to the structural properties indicating the high interest which has to be dedicated to beryllium oxide in microelectronics.

7. Conclusions

Our discussion was related to the improvement of the stability of tantalum base components. However the results deduced are of general importance, because the real structure is characteristic for most metal film arrangements and the interstitial impurity uptake and oxidizing ability are typical for many transition metals and alloys, the application of which in microelectronics is very progressive.

Based on our own experimental results we pointed out such modern aspects as epitaxial deposition or alloying of metal layers, doping of dielectric and insulating materials, and use of chemically stable thin film diffusion barriers. Higher stability could be reached by a combination of the different methods.

Tantalum-rhenium alloys and beryllium oxide are potential representatives of the introduced new film materials with applicable electronic properties.

BeO has many properties which allow us to conclude that this material should be able partially to remove such well known etchable diffusion barrier materials as SiO_2 , Si_3N_4 , and Al_2O_3 . Multivalent applications as dielectric in thin film capacitors, as insulating material at conductor crossing paths, and as piezoresistive material are conceivable.

This paper was sponsored by the VEB Keramische Werke Hermsdorf. Their continued support has contributed considerably to the results achieved. The authors wish gratefully to thank for this support.

References

- AUSTERMAN, S. B.: *J. Nucl. Mat.* **14**, 225 (1964)
 BERLINCOURT, T. G., BICKEL, P. W.: *Phys. Rev. B*, **2**, 4838 (1970)
 CHAO, K. A., ANSELL, G. S.: *J. appl. Physics* **41**, 417 (1970)
 CHOPRA, K. L.: *Thin Film Phenomena*, New York 1970
 COWGILL, M. G.: Thesis, University of Liverpool 1963
 COYNE, H. J., TAUBER, R. N.: *J. appl. Physics* **39**, 5585 (1968)
 DALTON, J. V., DROBEK, J.: *J. Electrochem. Soc.* **115**, 865 (1968)
 FRELLE, H., GÜNTHER, K. G.: *Thin Solid Films* **3**, 417 (1969)
 FROMM, E., GEBHARDT, E., ROY, U.: *Z. Metallkunde* **57**, 808 (1966)
 FROMM, E., HÖFER, G.: *Z. Metallkunde* **62**, 223 (1971)
 GOROŠENKO, Ja. T.: *Chimia Niobia i Tantala*, Kiev 1965
 GULBRANSEN, E. A., ANDREW, R.: *Trans. Met. Soc. AIME* **188**, 586 (1950)
 HACSKEYLO, M., SMITH, R. C.: *J. appl. Physics* **37**, 1767 (1966)
 HAUSNER, H. H.: *Beryllium — its Metallurgy and Properties*, Univ. of Calif. Press 1965
 HAUFFE, K.: *Reaktionen in und an festen Stoffen*, Berlin a. o. 1966
 HÖRZ, G.: *Metall* **22**, 1201 (1968)
 JANGG, G., KIEFFER, R., KÖGLER, H.: *Z. Metallkunde* **59**, 546 (1968)
 KRIVSKY, W. A.: *High Temperature Refractory Metals*, 1, New York, London, Paris 1968
 KOFSTAD, P.: *J. Elektrochem. Soc.* **109**, 776 (1962)
 KOFSTAD, P.: *J. Inst. Metals* **91**, 209 (1963)
 KOFSTAD, P.: *J. Less-Common-Met.* **7**, 241 (1964)
 LANGER, H.-D.: Thesis, Technische Hochschule Ilmenau 1970a
 LANGER, H.-D.: *Wiss. Zeitschrift der Technischen Hochschule Karl-Marx-Stadt* **12**, I (b) (1970)
 LANGER, H.-D.: *Diffusion in metallischen Werkstoffen*, Leipzig 1970c
 LANGER, H.-D.: in *Elektronenstruktur und physikalische Eigenschaften metallischer Werkstoffe*, Leipzig 1972, (d) Editor: H. Ringpfeil
 LANGER, H.-D., MEYER, S., SCHNEIDER, H. G.: in *Kristallisation metallischer Werkstoffe*, Leipzig 1969, Editor: H. Ringpfeil
 LEHOVEC, K.: *J. Less-Common Met.* **7**, 397 (1964)
 LEHOVEC, K.: *J. Electrochem. Soc.* **115**, 520 (1968)
 MAISSEL, L. I.: French Patent, Nr. 1353882, *Int. Class. H 01c* 1963
 MAISSEL, L. I., GLANG, R.: *Handbook of Thin Film Technology*, New York a. o. 1970
 MANASEVIT, H. M.: *Trans. Met. Soc. AIME* **236**, 275 (1966)
 MANASEVIT, H. M., FORBES, D. H., CADOFF, I. B.: *J. Metals* **17**, 701 (1965)
 MATTHEIS, L. F.: *Physic. Rev. A*, **139**, 1893 (1965)
 MATTHEISS, L. F.: *Physic. Rev. B*, **1**, 373 (1970)
 MEYER, S.: Thesis, Technische Hochschule, Ilmenau 1971
 MIRKIN, L. J.: *Spravočnik po rentgenostrukturnomu analisu polikristallov*, Moskva 1961
 MOHLER, D., HIRST, R. G.: *J. Electrochem. Soc.* **108**, 347 (1961)
 MÖNCH, S.: *Metall* **23**, 238 (1969)
 MORLEY, A. R., CAMPBELL, D. S.: *Thin Solid Films* **2**, 403 (1968)
 MÜLLER, H.: Thesis, Universität Freiburg 1958
 NORMAN, N.: *J. Less-Common Met.* **4**, 4 (1962)
 PAVLOVIĆ, A. S.: *J. Chem. Physics* **40**, 951 (1964)
 PÓCZA, J. F.: *In-situ Untersuchungen vakuumkondensierter dünner Schichten*, Paper, Symposium Kristallisation auf Oberflächen/Grundlagen der Epitaxie, Berlin 1969
 RIEB, G. D., VOGEL, D. L.: *Metalle für die Raumfahrt*, Reutte/Tirol 1965, Editor: F. Benešovsky

- SCHNEIDER, H. G., LANGER, H.-D.: *Wiss. Zeitschrift der Technischen Hochschule Ilmenau* **14**, 165 (1968)
 SCHÖNBERG, N.: *Acta Chem. Scand.* **8**, 240 (1954)
 SETO, D. K., BLAKESLEE, A. E.: *IBM Techn. Discl. Bull.* **9**, 922 (1966)
 SMYTH, D. M., SHIRN, G. A.: *J. Electrochem. Soc.* **115**, 186 (1968)
 SMYTH, D. M., TRIPP, T. B., SHIRN, G. A.: *J. Electrochem. Soc.* **113**, 100 (1966)
 STEEB, S., RENNER, J.: *J. Less-Common Met.* **10**, 246 (1966)
 STRINGER, J.: *J. Electrochem. Soc.* **112**, 1083 (1965)
 URASALIEV, U. S.: *Fis. Met. i Metallov.* **26**, 97 (1968)
 VERMILYEA, D. A.: *Acta Metallurgica* **6**, 166 (1958)
 YOUNG, L.: *Anodic Oxide Films*, London, New York 1961

(Received July 12, 1971;
 after revision October 15, 1971)

Author's address:

Prof. Dr. H. G. SCHNEIDER
 Dr. D. LANGER
 Technische Hochschule Karl-Marx-Stadt
 Sektion Physik-Elektronische Bauelemente
 90 Karl-Marx-Stadt
 PSF 964